

Supporting Information

PEG-based Cleavable Hydrogel Microparticles with controlled porosity for permiselective trafficking of biomolecular complexes in biosensing applications

Alessandra De Masi ^{a,b}, Pasqualina L. Scognamiglio ^{*a}, Edmondo Battista ^{*c}, Paolo A. Netti ^{a,b,c}, and Filippo Causa ^{a,b,c}

^a Center for Advanced Biomaterials for Healthcare@CRIB, Istituto Italiano di Tecnologia (IIT), Largo Barsanti e Matteucci 53, 80125 Naples, Italy

^b Dipartimento di Ingegneria Chimica dei Materiali e della Produzione Industriale (DICMAPI), University "Federico II", Piazzale Tecchio 80, 80125 Naples, Italy

^c Interdisciplinary Research Centre on Biomaterials (CRIB), Università degli Studi di Napoli "Federico II", Piazzale Tecchio 80, 80125 Naples, Italy

*Corresponding authors: P.L. Scognamiglio, pasqualina.scognamiglio@iit.it; E. Battista, edmondo.battista@unina.it

Table S1: Prepolymer solutions composition, in terms of PEGDA700 and DHEBA, and samples identification code.

NAME	PEGDA700 (w/v) %	DHEBA (w/v) %	R (mol PEG/mol Dheba)	X PEG	X DHEBA
15R40	15	0.1	42.9	0.98	0.02
15R4	15	1	4.29	0.81	0.19
10R40	10	0.07	40.8	0.98	0.02
10R4	10	0.7	4.08	0.81	0.19

Table S2: Flow rates and their ratio are imposed parameters; the capillary number Ca is calculated knowing the continuous phase properties and flow rate; mean droplet size and its standard deviation, frequency and spacing between two consequent droplets are obtained from the droplet generation videos analysis (Droplet Monitor software).

R	Q_d (μ L/min)	Q_c (μ L/min)	Size(μ m)	S.Dev.(μ m)	f (drops/s)	Spacing(μ m)	Ca
10	0.25	2.5	75	2.4	19.9	110.2	3.03E-02
10	0.5	5	70.3	6.5	38.6	101.2	6.07E-02
20	0.1	2.0	73.2	1.17	9.7	157.8	2.43E-02

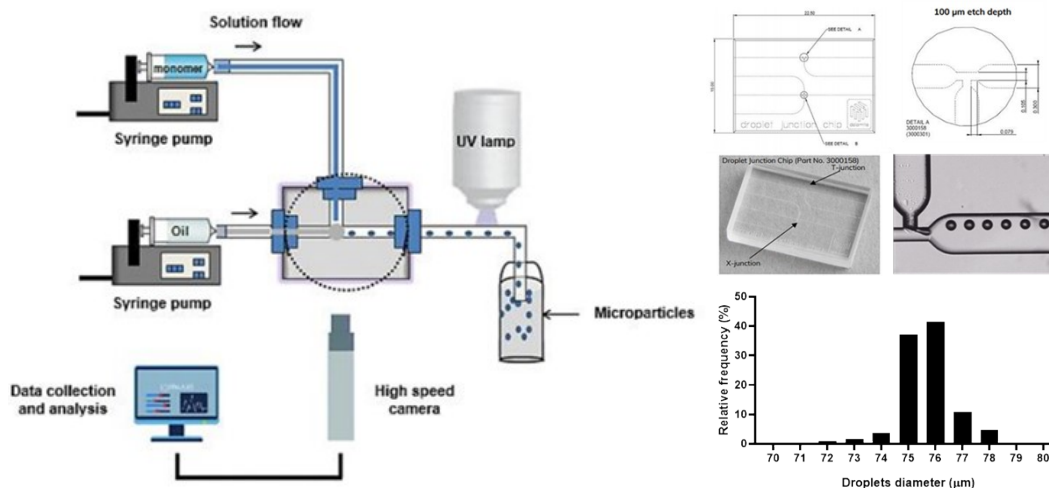


Figure S1: **Left:** Schematic illustration of the experimental microfluidic setup. Two syringe pumps push the solutions into the microfluidic channels, up to the T-junction where the droplet breakup occurs. Then the droplets are polymerized on flow in the outlet tube by means of an UV lamp and collected in a reservoir. A high-speed camera collects videos of the droplet formation and send the data to the software for the size and rate analysis; **Top Right:** Images and technical specification of the quartz hydrophobic droplet chip used for the W/O emulsion and an image of monodisperse droplets of 75 μm produced with the T-Junction chip; **Bottom right:** frequency distribution of droplets diameter evaluated from the video analysis of about 1000 droplets production (10R40).

Table S3: Microparticles' mean radius (μm) and standard deviation *pre-* and *post-* cleavage at 50 $^{\circ}\text{C}$ (overnight)

	Pre cleavage	Post cleavage
15R4	33.29 \pm 1.04	36.78 \pm 1.66
15R40	35.40 \pm 1.34	39.65 \pm 2.13
10R4	35.99 \pm 1.51	41.51 \pm 2.80
10R40	33.87 \pm 1.19	38.66 \pm 1.33

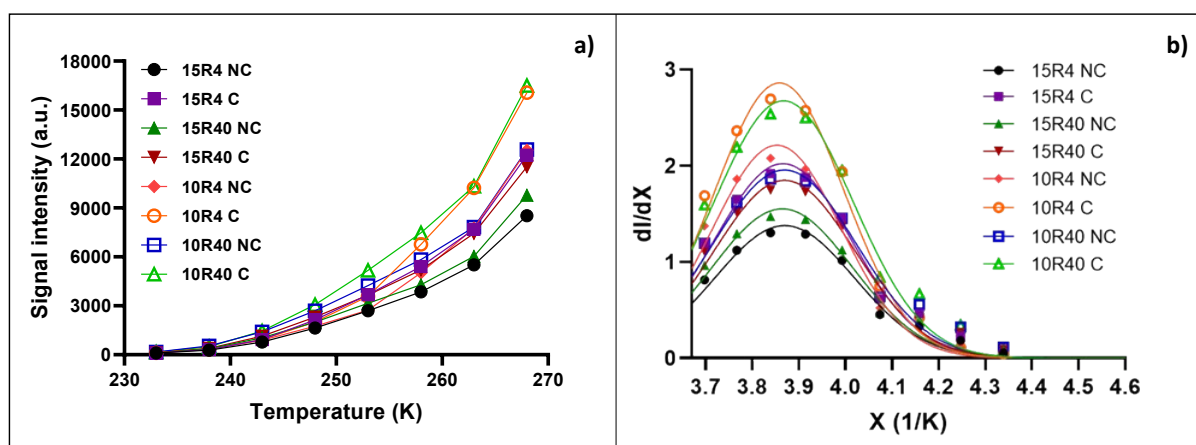


Figure S2: **a)** Variation of the NMR signal of water with the temperature for all the hydrogel compositions *pre-* and *post-* cleavage (IT curve); **b)** Derivative of the NMR signal with the inverse of temperature ($\text{K}^{-1} = X$, proportional to the pore radius) for all the hydrogel compositions.

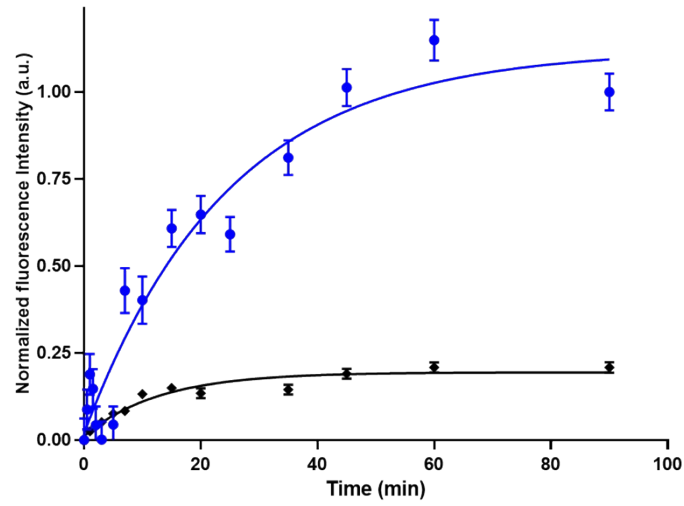


Figure S3: Diffusion kinetics of fluorescently labelled human IgG within 10R40 microparticles, before (black) and after the cleavage (blue).

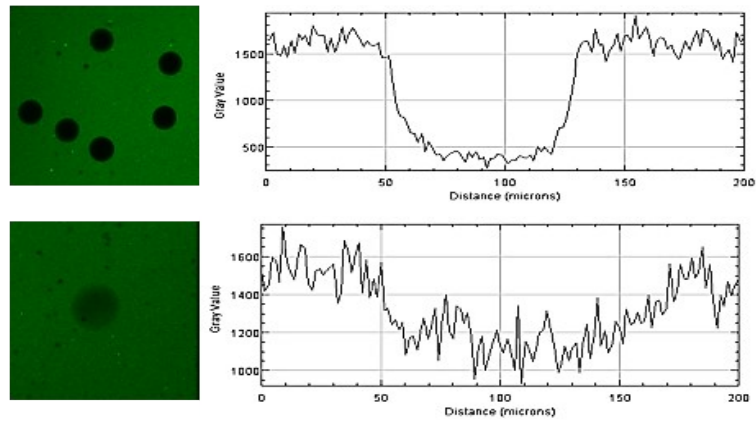


Figure S4: CLSM images and equilibrium fluorescence signal profile for the diffusion of a labelled IgG inside the 10R40 hydrogel microparticles, before (top) and after the cleavage (bottom);